ISSN 2394-3777 (Print)
ISSN 2394-3785 (Online)
Available online at www.ijartet.com

International Journal of Advanced Research Trends in Engineering and Technology (IJARTET)
Vol. 3, Issue 12, 2016 December

Characterization of Sputtered Nano-Au Layer Deposition on Silicon Wafer

Hsuan-Chao Hou [1], Yaser Mohammadi Banadaki [2], Srismrita Basu [3], Subhodip Maulik [4], Shu-Wei Yang [5], Safura Sharifi[6], Martin Feldman [7]

Dr. Hsuan-Chao Hou, Dept of ECE, Louisiana State University, Baton Rouge, USA [1]
Dr. Yaser Mohammadi Banadaki, Assist Pro, Dept of EE, Southern University and A&M College, Baton Rouge [2]
Mrs. Srismrita Basu, Dept of ECE, Louisiana State University, Baton Rouge, USA [3]
Mr. Subhodip Maulik, Dept of ECE, Louisiana State University, Baton Rouge, USA [4]
Mr. Shu-Wei Yang, Dept of Optics and Photonics, National Central University, Chungli, Taiwan (R.O.C.)[5]
Mrs. Safura Sharifi, Dept of ECE, Louisiana State University, Baton Rouge, USA [6]
Dr. Martin Feldman, Prof, Dept of ECE, Louisiana State University, Baton Rouge, USA [7]

Abstract: This paper reports a new technique to obtain the different nanostructures by sputtering system in place of costly lithographic steps. The morphologies of sputtered Gold (Au) metallic layers on silicon wafer had been measured by Alpha Step (D-100 KLA Tencor) atomic force microscopy AFM (NT-MDT Titanium AFM). While center position of the wafer with Au was roughly measured by Alpha Step, center to edge was measured precisely by AFM. Different Au thicknesses, average sizes, majority size ranges and detected particles with respect to the wafer positions were measured and discussed in this paper. In this paper, we found a pattern to fabricate thicknesses and sizes of nano Au structure from 6.6 nm to 17.9 nm and from 23.4 nm to 44.3 nm. Moreover, the Au particle could be deposited with a certain angle without tilting either a target or substrate. The different numbers and sizes of Au particles per surface deformations with craters and rims on different positions were caused by speculated factors, deposition angles and positions.

Keywords: Sputtered, Positions, Thicknesses, Detected Au particles, AFM, cluster, and Au Nano-Islands (AuNIs).

I. INTRODUCTION

A uniform thin film deposition technology stands a significant place in microelectromechanical (MEMs) technology for sensors, actuators, transducers and energy harvesting [1-3]. Nowadays, there are two main categories for fabricating a metallic thin film: chemical deposition and physical depositions. In this paper, sputtering deposition method (PVD), the method of dynamic atoms pass through a low pressure gas and condense on the substrate, was operated instead of chemical deposition (CVD), chemical reactions between the substrate surface and reactant gases. The following reasons are the low deposition temperature protects the substrate from damage, Au small grain size is widely employed for nano structure applications, the low impurity film increases signal strength, the bulk fabrication makes the competitive price.

Aluminum (Al), Gold (Au), Copper (Cu), and Silver (Ag) are the common materials for the thin metallic layers by MEMs deposition methods. In the majority of applications, Au metal is chosen due to nontoxic metal as silver (Ag), nonreactive with other materials especially oxygen, high reflectance and almost transparent in thin film for optical applications, high etching selectivity, and good conductivity for better signal strength. Publication had shown the morphologies of Au metallic layers with different deposition methods. For example: An average size 22 nm and roughness of 50 nm of Au nano islands (AuNIs) on the microscope glass were fabricated by thermal evaporator and thermal annealing (700 °C) processes. In addition, an average size of 10 nm to 50 nm partially embedded gold nano-islands with 4.5 nm initial thick gold film on a microscope glass slide were fabricated by high-end precision electron beam evaporator and followed with 500 °C thermal annealing processes [4, 5]. Those results show that the shapes of AuNIs and the distance between each AuNIs could be manipulated by deposition and annealing times[6]. However, the majority of the discussions are all focused on the center area of the deposition. In this paper, the thicknesses, particle sizes will be measured by AFM from center to the edge.

ISSN 2394-3777 (Print)
ISSN 2394-3785 (Online)
Available online at www.ijartet.com

International Journal of Advanced Research Trends in Engineering and Technology (IJARTET)
Vol. 3, Issue 12, December 2016

II. EXPERIMENTAL

John S. Chapin invented the first planar magnetron sputtering source with a magnetic field to manipulate the velocity and behavior of charged ions and electrons in 1974. Charged ions are trapped in a magnetic field toward the target in order to increase the deposition rates. Technical problems such as slow deposition rate, substrate overheat, and small substrate coverage were overcame by this novel invention, by upgrading the conventional diode sputtering [7]. Most magnetron cathodes are rectangular or circular. Rectangular magnetrons are more commonly used with larger substrates; while circular magnetrons are more commonly used with smaller substrates. Three main power sources inducing the high energy state of magnetrons sputtering are direct current (DC), alternating current (AC) and radio frequency (RF) magnetron sources. The DC powered circular magnetron sputtering chamber (Oxford Plasmalab System 400 Sputtering System in CAMD center for advanced microstructures & devices) was employed in this paper for Au deposition. In this paper, the Au deposition was performed inside the sputtering chamber in figure 1(a). Inside the 15 cm in diameter chamber, a 7.5 cm in diameter Au target was connected to a negative voltage on the top, while a 10 cm long stage was connected to the ground at the bottom. On this stage, a 14 cm long aluminum sample was attached to a 4 inch Silicon wafer and placed 10 cm from the Au target. The purpose that the size of the sample was longer than the Au target and the stage was to analyze the different characterizations of Au deposition from center to edge. The Au structures on the sample were not fully connected to each other due to the thin atomic deposition of Au. A simulation of sputtered Au emitted toward the substrate formed clumpy cluster was presented [8]. Figure 1(b) illustrates the principle of sputtering deposition with a high vacuum 10^{-6} Torr and argon gas inside the chamber. A negative DC voltage is applied to the argon gas creating a neutral plasma that contains free electrons and ionized argons. The free electrons are accelerated away from the Au target (cathode) by the negative electrical potential. The positive argon ions are accelerated toward the Au target bombarding the Au atoms (the radius of Au atom is 0.1441 nano-meter). Consequently, neutral Au atoms are ejected from the Au target and deposited on the grounded substrate. When the free electrons recombine with the positive argon ions, photons are emitted, introducing the deep purple color of plasma. The deposition rate remains constant until the desired thickness is achieved.

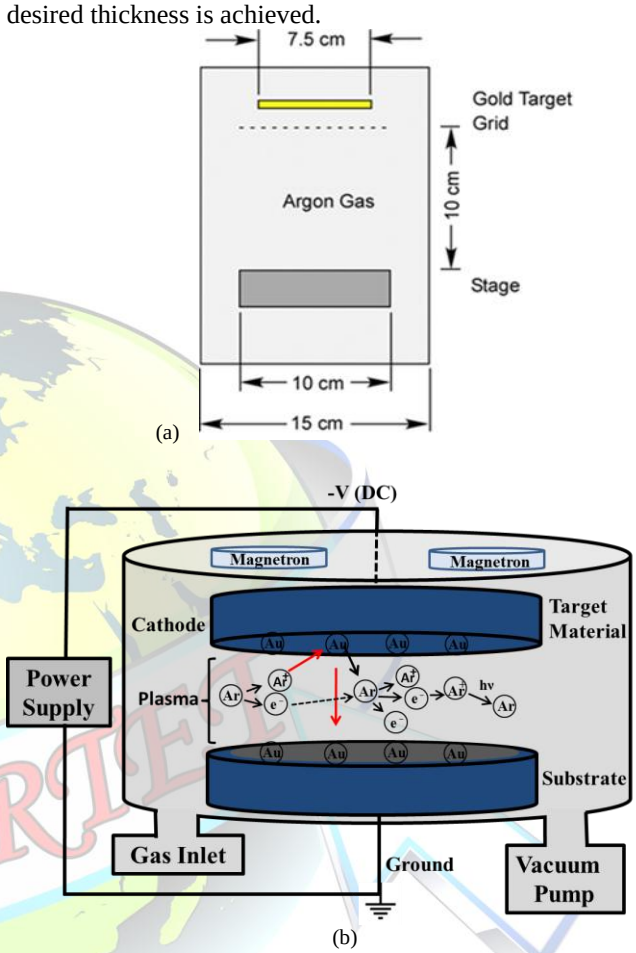

Fig. 1. (a) The dimensions of the DC powered magnetron sputtering system. (b) Schematic principle of DC powered magnetron sputtering system. [9]

A 14 cm length of the aluminum foil substrate (2 sets of 7 cm strips) was placed inside the sputtering chamber shown in figure 2 (a) in order to verify the color changed before and after deposition. After Au deposition, the symmetric colors of the Au on aluminum substrates were violet, blue, light green, yellow, light green, blue and violet from edge to center and from center to edge (-7 cm to 7 cm) shown on figure 2 (b). The color distribution shows that the Au was evenly disturbed on the center and gradually changed toward to the edges. The size, thickness, and structure of Au particles on the aluminum substrate were assumed to be the

ISSN 2394-3777 (Print)
ISSN 2394-3785 (Online)
Available online at www.ijartet.com

International Journal of Advanced Research Trends in Engineering and Technology (IJARTET)
Vol. 3, Issue 12, December 2016

same as Au structure on the wafer, because the wafer and aluminum foil substrate were processed simultaneously, so the amount of Au deposition at each position should be the same.

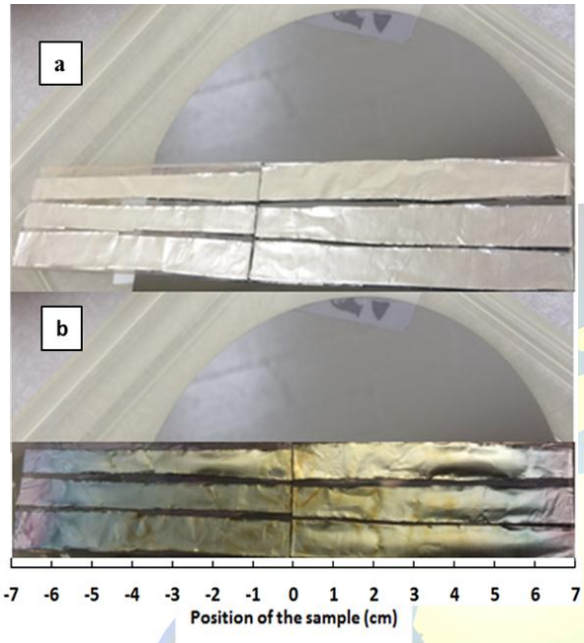

Fig. 2. Sputtered Au on wafer and three aluminum substrates (Position of the sample -7 cm to 7cm) (a) before, (b) after Au deposition.[9]

III. RESULTS

A. *Center (Position of the sample: 0~2 cm)*

In this research, an Au thin film (figure 3) was deposited on a smooth side of the wafer by the DC powered magnetron sputtering system under 450 mA for 430 seconds. The average thickness of sputtered Au on the center of the wafer was roughly around 20 nm measured by Alpha Step. The partially 80 nm thickness was caused by the thickness of the microscope slide on the wafer. A microscope slide was place on the wafer during the Au deposition, then it was removed during the thickness measurement, so accumulated 80 nm Au were observed.

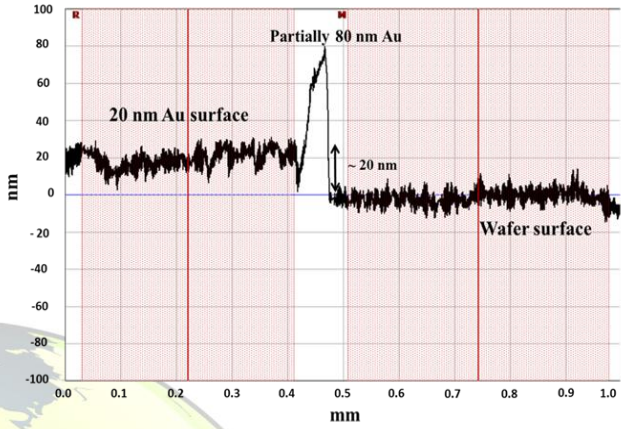

Fig. 3 20 nm Au thin film on the center of the smooth side wafer was fabricated by DC powered magnetron sputtering system and measured by Alpha Step.[9]

B. *Edge toward to the center (Position of the sample: 7 cm to 2 cm)*

At the position of the sample (6 cm to 7 cm) shown on figure 4, the AFM images shows that a 6.6 nm Au thickness with a majority size range from 10~ 25 nm Au particle sizes (average 23.4 nm with standard deviation 8.3 nm), and 1043 Au particles per μm^2 area are detected. This edge of the chamber position produces the thinnest Au layer, which contains the smallest and maximum number of Au particles compare to the other position.

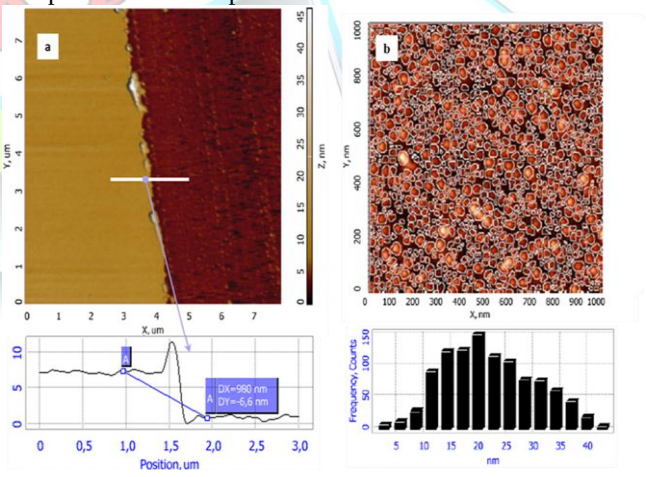

Fig. 4 The AFM images at 6~7 cm position (a) Au thickness on the wafer, (b) detected Au particle sizes and numbers [1 µm × 1 µm field of view].[9]

ISSN 2394-3777 (Print)
ISSN 2394-3785 (Online)
Available online at www.ijartet.com

International Journal of Advanced Research Trends in Engineering and Technology (IJARTET)
Vol. 3, Issue 12, December 2016

At the position of the sample (5 cm to 6 cm) shown on figure 5, the Au thickness was 8.1 nm with a majority size range 20~ 45 nm Au particle sizes (average 31.7 nm with standard deviation 11.3 nm), and 640 Au particles per μm^2 area are detected. At this point, the Au clumps accumulated into bigger and thicker clumps compared to the previous position (6 cm to 7 cm), so that the number of the detected Au particles decreased toward to the center.

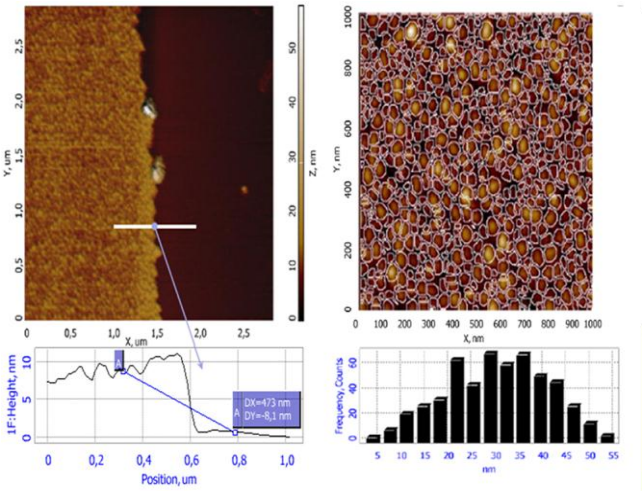

Fig. 5 The AFM images at 5~6 cm position (a) the Au thickness on the wafer, (b) the detected Au particle sizes and numbers [1 µm × 1 µm field of view].[9]

At the position of the sample (4 cm to 5 cm) shown on figure 6, the Au thickness was 14 nm with a majority size range 30~60 nm Au particle size (average 44.3 nm with standard deviation 15.3 nm) and 323 Au particles per μm^2 area are detected. This spot produced larger Au particle size and wider particle size range compared to the previous position (5 cm to 6 cm). At this point, the Au clumps accumulated into the biggest and thickest clumps with the least the number of the Au particles compared to all the positions.

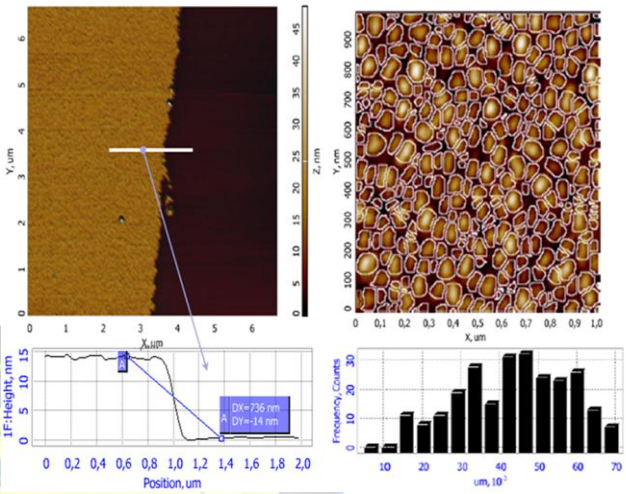

Fig. 6 The AFM images at 4~5 cm position (a) the Au thickness on the wafer, (b) the detected Au particle sizes and numbers [1 µm × 1 µm field of view].[9]

At the position of the sample (3 cm to 4 cm) shown on figure 7, Au thickness was 15.4 nm with a majority size range 15~ 35 nm Au particle sizes (average 28.3 nm with standard deviation 8.8 nm), and 666 Au particles per μm^2 area are detected. At this point, the Au clumps accumulated into thicker clumps but it shrunk on the size compared to the previous position (4 cm to 5 cm), but the number of the Au particles started increasing toward the center.

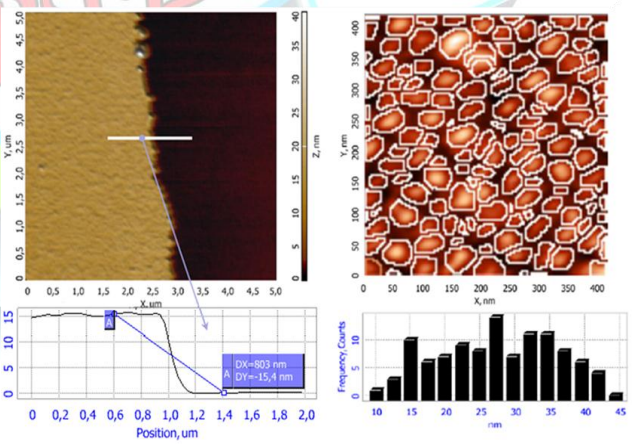

Fig. 7 The AFM images at 3~4 cm position (a) the Au thickness on the wafer, (b) the detected Au particle sizes and numbers [0.45 µm × 0.45 µm field of view].[9]

ISSN 2394-3777 (Print)
ISSN 2394-3785 (Online)
Available online at www.ijartet.com

International Journal of Advanced Research Trends in Engineering and Technology (IJARTET)
Vol. 3, Issue 12, December 2016

At the position of the sample (2 cm to 3 cm) shown on figure 8, Au thickness was 17.9 nm with a majority size range 15~ 40 nm Au particle sizes (average 29.7 nm with standard deviation 9.6 nm) and 625 Au particles per μm^2 area are detected. At this point, the Au clumps accumulated thicker clumps, but compared to the previous position (3~4 cm) the size and the number of Au particles remain the same.

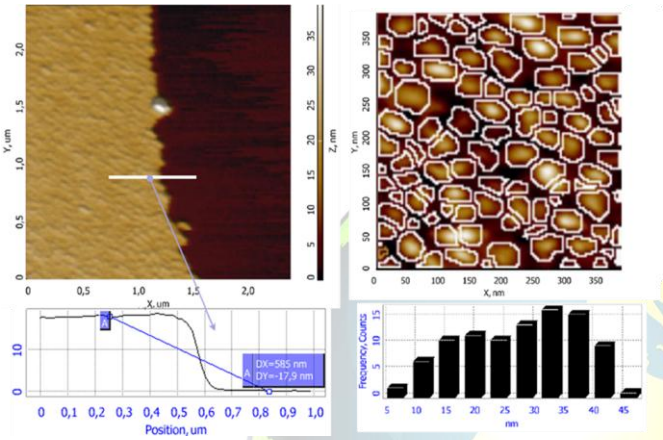

Fig. 8 The AFM images at 2~3 cm position (a) the Au thickness on the wafer, (b) the detected Au particle sizes and numbers [0.4 µm × 0.4 µm field of view].[9]

IV. SUMMARY AND DISCUSSION

The AFM measurements in figure 9 and table 1 show that the distribution of the Au thicknesses, particle sizes and detected particles on the wafer with respect to the position from 2 cm to 7 cm. The Au thicknesses from center to edge linearly decrease from 17.9 to 6.6 nm, whereas the thickness near the center was 17.9 nm which is more or less same as the measurement in figure 2.1. However, the average sizes of the Au particle, with more less the same standard deviation, can be divided into four regions. At region I , Au particle sizes 29 nm were remained the same around the center from 2 to 4 cm area where produced roughly the same number of Au particles (625 verses 666) and majority size range (15nm~ 40nm verses 15 nm~ 35 nm). At region II, then, Au particle size increased to 44.3 nm at 4 to 5 cm area where produced less Au particles (323) and wider majority size range (30nm ~ 60nm). At region III, Au particle sizes linearly decreased toward the edge from 44.3 nm to 23.4nm. The conclusion is that the Au thicknesses linearly decrease from center to edge, but not for the size of the Au particle.

In this paper, all the date is analyzed based on the measurement results. The different numbers and sizes of Au particles per surface deformations with craters and rims from center to edge are caused by speculated factors, deposition angles based on different positions. The distribution of sputtered Au nanoparticles has been studied by using molecular dynamics simulations: For a spherical Au target, the sputtered Au is emitted isotopically [10]. For our system planar Au target, the majority of the sputtered Au is emitted toward the substrate [11]. The Au deposition angles can be divided into three directions: 1. Majority of Au particle, vertically emitted from the Au target, is deposited on the center area (2 cm to 4cm, region I), where the Au clumps accumulate and stack up into thicker Au clumps with the consistent deposition. 2. The minority of the Au particle, rebounded from the wall with certain angles, fills up the gap between each clumps on the area (4 cm to 5 cm, region II), where produces smallest number, wider size range, and largest Au particle. 3. The minority of the Au particle, directly emitted from the Au target with certain angles, is deposited on the edge area (5 cm to 7cm, region III), where produce largest number, narrow size range, and smallest Au particle due to the minority numbers.

It means that the sputtered Au can be deposited with certain angles based on second and third statements. Glancing angle deposition is a powerful technique which has been widely utilized for physical vapor deposition [12, 13]. Sputtered Au structures at certain angles normal to the substrate have been fabricated by tilting the angle of substrate during deposition [14]. Alternative method is to adjust the angles of Au deposition during sputtering produced the same structure instead of tilting the angles of substrate [15]. In this paper, we found another method to achieve the same goal instead of tilting either target or substrate. It will be doable to employ other metallic materials and follow or transfer this fabrication processed pattern to other cost deposition devices such as thermal evaporate, chemical vapor deposition, and electroplating in order to investigate or achieve desirable nano-particle sizes, thicknesses, majority size ranges, and numbers for nanotechnology applications such as environmental filters, nano-optics, high energy density batteries, high-sensitivity biomedical sensors, nanocomposite and high power magnets.

ISSN 2394-3777 (Print)
ISSN 2394-3785 (Online)
Available online at www.ijartet.com

International Journal of Advanced Research Trends in Engineering and Technology (IJARTET)
Vol. 3, Issue 12, December 2016

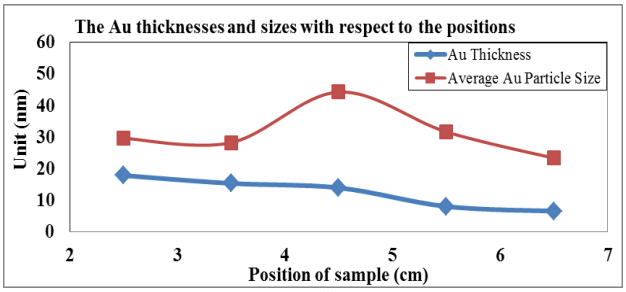

Fig. 9 Au thicknesses on the wafer with respect to position (2 cm to 7cm).

TABLE I

TABLE 1 THE COMPARISON OF AU CHARACTERISTICS ON THE WAFER WITH RESPECT TO THE POSITIONS.

Region	I		II	III	
Position (cm)	2~3	3~4	4~5	5~6	6~7
Thickness (nm)	17.9	15.4	14	8.1	6.6
Average Size (nm)	29.7	28.3	44.3	31.7	23.4
Majority Size Range (nm)	15~40	15~35	30~60	20~45	10~25
Detected Particles $(\mu m^2)^{-1}$	625	666	323	640	1043
SD (nm)	9.6	8.8	15.3	11.3	8.3
SD%	32%	31%	34.5 %	35.6%	35.4

REFERENCES

[1]. P. Muralt, R. Polcawich, and S. Trolier-McKinstry, "Piezoelectric thin films for sensors, actuators, and energy harvesting," *MRS bulletin*, vol. 34, pp. 658-664, 2009.

[2]. A. Hajati, D. Latev, D. Gardner, M. Ottosson, D. Imai, M. Torrey, *et al.*, "Monolithic ultrasonic integrated circuits based on micromachined semi-ellipsoidal piezoelectric domes," *Applied Physics Letters*, vol. 103, p. 202906, 2013.

[3]. A. Hajati and S.-G. Kim, "Ultra-wide bandwidth piezoelectric energy harvesting," *Applied Physics Letters*, vol. 99, p. 083105, 2011.

[4]. S.-U. Fang, C.-L. Hsu, T.-C. Hsu, M.-Y. Juang, and Y.-C. Liu, "Surface roughness-correlated SERS effect on Au island-deposited substrate," *Journal of Electroanalytical Chemistry*, vol. 741, pp. 127-133, 2015.

[5]. M. T. Yaseen, M. Chen, and Y.-C. Chang, "Partially embedded gold nanoislands in a glass substrate for SERS applications," *RSC Adv.*, vol. 4, pp. 55247-55251, 2014.

[6]. Z. Kang, J. Chen, S.-Y. Wu, K. Chen, S.-K. Kong, K.-T. Yong, *et al.*, "Trapping and assembling of particles and live cells on large-scale random gold nano-island substrates," *Scientific reports*, vol. 5, 2015.

[7]. P. S. McLeod, "Planar magnetron sputtering method and apparatus," ed: Google Patents, 1976.

[8]. S. Zimmermann and H. M. Urbassek, "Sputtering of nanoparticles: Molecular dynamics study of Au impact on 20nm sized Au nanoparticles," *International Journal of Mass Spectrometry*, vol. 272, pp. 91-97, 2008.

[9]. H.-C. Hou, "Nano Cost Nano Patterned Template for Surface Enhanced Raman Scattering (SERS) for IN-VITRO and IN-VIVO Applications," Louisiana State University, 2016.

[10]. R. Kissel and H. M. Urbassek, "Sputtering from spherical Au clusters by energetic atom bombardment," *Nuclear Instruments and Methods in Physics Research Section B: Beam Interactions with Materials and Atoms*, vol. 180, pp. 293-298, 6// 2001.

[11]. G. Falcone, "Sputtering yield including anisotropic effects," *Physics Letters A*, vol. 129, pp. 188-190, 1988.

[12]. J. Wang, H. Huang, S. Kesapragada, and D. Gall, "Growth of Y-shaped nanorods through physical vapor deposition," *Nano letters*, vol. 5, pp. 2505-2508, 2005.

[13]. M. M. Hawkeye and M. J. Brett, "Glancing angle deposition: fabrication, properties, and applications of micro-and nanostructured thin films," *Journal of Vacuum Science & Technology A*, vol. 25, pp. 1317-1335, 2007.

[14]. J. M. García-Martín, R. Alvarez, P. Romero-Gómez, A. Cebollada, and A. Palmero, "Tilt angle control of nanocolumns grown by glancing angle sputtering at variable argon pressures," *Applied Physics Letters*, vol. 97, p. 173103, 2010.

[15]. H. Tsuge and S. Esho, "Angular distribution of sputtered atoms from polycrystalline metal targets," *Journal of Applied Physics*, vol. 52, pp. 4391-4395, 1981.

BIOGRAPHY

Hsuan-Chao Hou gained his Ph.D. this summer 2016. Currently, he is a research assistant at Electrical & Computer Engineering at Louisiana State University, Baton Rouge. His current research interests include MEMs fabrication for bio-sensors with focusing on metallic nano-structure, thin film, imaging (AFM, SEM) Raman enhancement, optical design, optical fiber and bio-applications.